On the direct measurement of the adiabatic temperature change of magnetocaloric materials

Journal of Applied Physics

AIP Publishing

On the direct measurement of the adiabatic temperature change of magnetocaloric materials

F. Cugini[a,b,*] and M. Solzi[a,b]

[a] *Department of Mathematical, Physical and Computer Sciences, University of Parma, Parco Area delle Scienze 7/A 43124 Parma, Italia.*
[b] *IMEM-CNR Institute, Parco Area delle Scienze 37/A 43124 Parma, Italia.*
**francesco.cugini@unipr.it*

Abstract

The direct measurement of the adiabatic temperature change of magnetocaloric materials is fundamental to design efficient and eco-friendly magneto cooling devices. This work reports an overview of the measurement principle and of the main experimental issues that have to be considered to obtain a reliable characterization of materials. The effect of non-ideal adiabatic conditions, the role of the temperature sensor and the influence of specific properties of the material are discussed on the basis of finite-difference thermal simulations and special designed experiments. Two cases are considered in detail: the characterization of thin samples and the measurement of caloric response to fast field changes. Finally, the impact of different measurement protocols is discussed in the case of materials with first-order transitions.

1. Introduction

Refrigeration plays a fundamental role in our modern society: it permeates our life and contributes to the evolution and the wellness of humanity. However, it costs more than the 18% of the global energy consumption and this number is constantly increasing duo to the diffusion of refrigeration technologies in developing countries. [1] This large demand of energy and the high environmental impact of the actual gas-compression systems make urgent the promotion of new eco-friendly solutions. Among the emergent technologies, there is the magnetic refrigeration, which promises a low ecological impact, no hazardous fluids, high efficiency and reduced electrical energy consumptions. [2] Magnetic refrigeration is based on the magnetocaloric effect (MCE), that consists of an adiabatic temperature change (ΔT_{ad}) or an isothermal entropy change (Δs_T) induced in a magnetic material by a variation of an applied magnetic field. [3] By a cyclical variation of the magnetic field a refrigerant cycle is obtained. [2] Four elements are essential to build a magnetic cooling system: a magnetocaloric (MC) material, a source of magnetic field, a mechanism to move the material relative to the field and a fluid for the heat transfer. The temperature change induced in the MC material by the application or removal of magnetic field is the driving force that leads the heat transfer. It depends on the properties of the material and on the strength of the applied magnetic field. Currently, the most promising MC materials show a reversible ΔT_{ad} of about 3 K in a magnetic field change of 1 T, that is achievable with an assembly of permanent magnets. [4–6]

Though many prototypes of magnetic refrigerator were built in the last two decades, the development of competitive MC devices still demands more performing MC materials and new smart technical solutions. [2,4,7] Besides the basic investigation of magnetic properties of materials, the search for efficient cooling elements requires the measurement of their MC

performance. In particular, the direct characterization of the adiabatic temperature change is essential to design and optimize magnetic cooling elements, by directly testing their thermodynamic response to the magnetic stimulus. [4] A direct adiabatic temperature change measurement requires an experimental setup that can record the sample temperature change induced, in adiabatic condition, by varying an applied magnetic field. Though this procedure looks simple, the measurement of the adiabatic temperature change is not always reported in the literature on MC materials, differently from the isothermal entropy change, due both to the lack of available commercial instruments and to the fact that obtaining reliable measurements is not at all obvious. In the last decades many experimental setups have been developed. The temperature of the sample is usually measured with standard temperature sensors (thermocouples [8–15] or high precision thermoresistances [16,17]). Whereas, the change of the magnetic field is achieved by turning on and off an electromagnet or a superconductive magnet [8,13,14,17,18] or by moving the sample relative to a field source [9,15–17] or by exploiting pulsed magnetic fields. [8,11,19,20] Special sample holders were designed to reduce the heat-exchange between the sample and surroundings during the measurement, thus reproducing nearly-adiabatic conditions. [9,18] Moreover, some experimental setups based on non-contact measurements techniques, like thermoacoustic methods, [21,22] the detection of IR-radiation [18,23,24] and thermo-optical techniques [20,25] have also been proposed for the characterization of MCE in particular conditions. Though good levels and a wide diversification of experimental solutions have been obtained, a comprehensive analysis of the main issues that can affect an adiabatic temperature change measurement and the interpretation of its results is still lacking.

This manuscript reports an overview on the principle of the adiabatic temperature change measurement and on the main experimental issues that have to be considered to design the experiment and to obtain a reliable characterization of the MCE. The effect of non-ideal adiabatic conditions, the role of the temperature sensor and the influence of material properties are discussed on the basis of experimental measurements and finite-difference heat transfer simulations. Two critical cases are analysed in detail: the characterization of samples with a small thermal mass and the measurement of the MCE induced by fast field changes. The direct measurement of MCE of microstructured materials is fundamental to design active MC elements with a large surface to volume ratio [2] or innovative micro or miniaturized solid-state devices. [26,27] Indeed, it was demonstrated that mechanical processing or thermal treatments, due to particular synthesis routes or post-synthesis manufacturing, can drastically change the functional properties of some MC materials. [28–31] Whereas, the measurement of the MCE induced by fast field changes is important to: (a) test the dynamic response of MC materials, thus evaluating possible kinetic effects of magnetic transitions, (b) rapidly check the performances of materials subjected to continuous and repeated thermomagnetic cycles, (c) study the MCE induced by very large magnetic fields and (d) measure the adiabatic temperature change of very thin samples.

The paper is divided in 4 paragraphs. Paragraph 2 outlines the basics of ΔT_{ad} measurement and describes the model utilized to perform finite-difference heat transfer simulations and the instrument exploited to obtain the experimental data that are reported in the following. In paragraph 3 the effect of non-ideal adiabatic conditions, which are a critical aspect especially in the case of samples with a small thermal mass, are discussed. Paragraph 4 is devoted to the analysis of the role of temperature sensor and of the thermal contact with the sample. Subparagraph 4.1 is focused on the effect of the sensor thermal mass, which becomes relevant when it is comparable with that of the sample. The different experimental solutions that have

been proposed to measure thin samples are discussed. Subparagraph 4.2 deals with the effect of the response time of temperature sensor, which depends on its thermal capacitance and on the sensor-sample thermal contact conductance. In particular, the critical issues in the measurement of the MCE induced by pulsed magnetic fields are treated. A review of the main experimental setups that exploit a pulsed magnetic field is reported together with outcomes of thermal simulations that display possible artefacts in the measurement, due to the slow response time of temperature sensor. Finally, paragraph 5 deals with the effect on the ΔT_{ad} measurements of the sample thermal conductivity and of the peculiarities of the magnetic transition, at which the MCE occurs. Different measurement protocols are described and the expected outcomes are discussed on the basis of available literature and measurements performed on a Heusler sample that shows both a second-order and a first-order magnetic transition.

2. Measurement principle and experimental details

The direct characterization of the adiabatic temperature change of a MC material is usually performed by measuring the sample temperature during the application or the removal of an external magnetic field with the sample kept in nearly-adiabatic conditions. Three elements are required: (1) a thermometer to measure the sample temperature, (2) a source of a variable magnetic field or a mechanical system to move the sample relative to a static field source and (3) a sample holder that ensures adiabatic conditions. Figure 1 shows a schematic illustration of a system to directly measure the adiabatic temperature change and the equivalent electrical circuit. The sample is characterized by a heat capacity C_s and a temperature T_s. In the equivalent electrical circuit, the MCE is represented as a current source, in parallel with the capacitance that corresponds to the sample. [32] The sample is in contact with the temperature sensor, characterized by a heat capacity C_t and a temperature T_t. The thermal contact between the sample and the sensor, that depends on various factors and it is normally improved using a thermoconductive paste, is taken into account through the total thermal conductance $K_{s\text{-}t}$. The heat exchange between the sample-sensor system and the surroundings, that is, at the temperature T_e, is schematized with the thermal conductances $K_{s\text{-}e}$ (sample-environment) and $K_{t\text{-}e}$ (temperature sensor-environment).

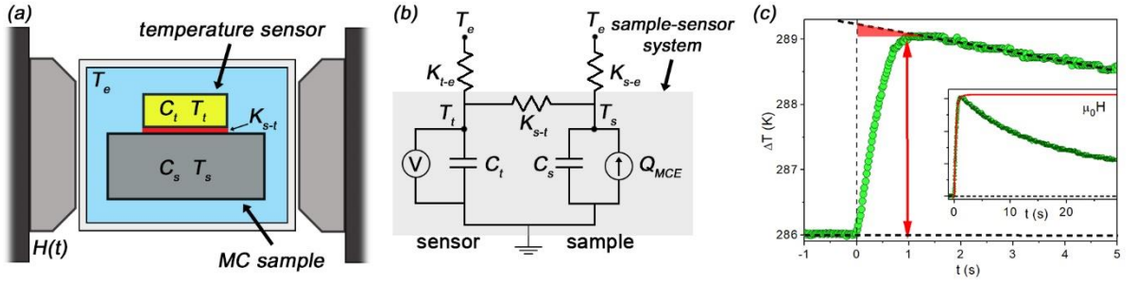

Figure 1 (a) Schematization of an experimental system to directly measure the adiabatic temperature change. (b) Equivalent electrical circuit. (c) Example of a direct ΔT_{ad} measurement of a Gd sample performed by applying a magnetic field of 1.8 T. Inset: $\Delta T_{ad}(t)$ on an extended time scale.

The temperature change of the sample, induced by a variation of the applied magnetic field (ΔH), is measured through the thermometer. Under ideal conditions, the sample and the sensor are constantly in thermal equilibrium ($K_{s\text{-}t} = \infty$) and the heat exchange between the sample-sensor system and the surroundings is zero ($K_{t\text{-}e}$ and $K_{s\text{-}e} = 0$). In these conditions, by measuring the thermometer temperature as a function of time $T_t(t)$ during a field variation we can directly obtain the ΔT_{ad} of the sample. However, the experimental achievement of accurate ΔT_{ad} measurements requires the careful evaluation of some specific issues: (a) the adiabatic condition, (b) the role of the temperature sensor and (c) the effect of specific properties of the material. In the following paragraphs these aspects will be analysed through thermal simulations and experimental results. The simulations, based on the finite-difference method, were performed by considering the schematic configuration of the experimental setup that is reported in Figure 1.a. Some variations of the model were considered to account different effects that can modify the measurement. The experimental measurements were obtained by the setup described in Ref. 17. This instrument is based on a thermoresistance, a Cernox bare chip, characterized by a mass of 3 mg, a response time of 0.135 s and a very low sensitivity to magnetic field. The resolution of the temperature sensor, limited by the electronic noise, is of 0.07 K. The sample is placed in contact with the back side of the temperature sensor through a thermoconductive paste (thermal conductivity ~ 7 $Wm^{-1}K^{-1}$). The magnetic field variation is obtained by turning on and off a low inductive electromagnet or by moving in and out from the electromagnet, through a pneumatic piston, the probe containing sample and sensor. In the first case, a maximum field change of 1.9 T can be achieved in 1 s (average field sweep rate: 1.8 T s^{-1}). Instead, by using the pneumatic piston, which is characterized by a running time of 0.15 s, a maximum average magnetic field sweep rate of 10 T s^{-1} is reached.

3 Adiabatic conditions

The first aspect that has to be evaluated is the achievement of adiabatic condition, by decreasing as much as possible the heat transfer between sample and environment during the application of the magnetic field. The heat exchange with the surroundings can be prevented by reducing the thermal contact between sample and sample-holder and by using a vacuum environment and radiation shields ($K_{s\text{-}e} \rightarrow 0$). However, a complete thermal insulation of the sample is in contrast with the necessity to change, control and stabilize its temperature before the ΔT_{ad} measurement. A compromise has to be found between these two opposite requests. Alternatively, another way to decrease the heat dissipated during the measurement is to perform fast measurements by using fast magnetic field changes: by reducing the measurement time, also the heat dissipated from the sample is reduced. Mechanical systems that move the sample relative to a region with a static magnetic field or pulsed magnetic fields can be utilized to achieve this aim [8,17]. However, the reduction of the measurement time introduces new problems related to the response time of temperature sensor (described in details in paragraph 4.2).

In general, the quality of adiabatic conditions rules, together with the resolution of temperature sensor, the error related to the measurement. Figure 1.c shows an example of a ΔT_{ad} measurement of a Gd sample performed by applying a magnetic field change of 1.8 T in 1 s. By extrapolating the temperature behaviour after the field application, due to the heat dissipated to the environment, it is possible to estimate the error introduced by the non-ideal adiabatic conditions (highlighted by the red triangle). However, an accurate determination of the error

associated to the heat exchanged during the measurement is not at all simple, considering the variation of sample temperature. In general, we can assume that the ΔT_{ad} error rises by increasing the temperature change, which improves the sample-environment heat exchange, and by reducing the thermal capacitance of the measured sample ($C_s = m_s c_s$).

$$err_{\Delta T} \propto \frac{\Delta T_{ad} \cdot K_{s-e}}{m_s c_s} \qquad (1)$$

This approximated equation highlights that non-ideal adiabatic condition has a not negligible effect specially in the case of samples with a small thermal mass, as thin sheets, ribbons or in general micro-structured samples. This effect was experimentally verified in Ref. 18 by measuring through a non-contact temperature sensor the adiabatic temperature change of a Gd thin sheet as a function of its progressively reduced thickness. A special designed sample holder was utilized to minimize the conductive and convective heat dissipation. The authors demonstrated that the main contribution to heat dissipation, during the ΔT_{ad} measurement, is the thermal radiation. Figure 2 reports the difference, as a percentage, between the measured ΔT_{ad} and the intrinsic ΔT_{ad} of the sample. The observed error is caused by the heat dissipated, as thermal radiation, during the measurement. Its increase, by decreasing the thickness of the sample, is due to the decrease of the sample mass, as reported in Equation 1. Finite-difference simulation of the thermal system, performed by considering only irradiation as heat dissipation, results in the same trend of experimental data. By extending this simulation, the authors of Ref. 18 demonstrated that the only solution to obtain a reliable direct measurement of ΔT_{ad} in very thin samples is to reduce the duration of the measurements, by decreasing the characteristic time of the field change.

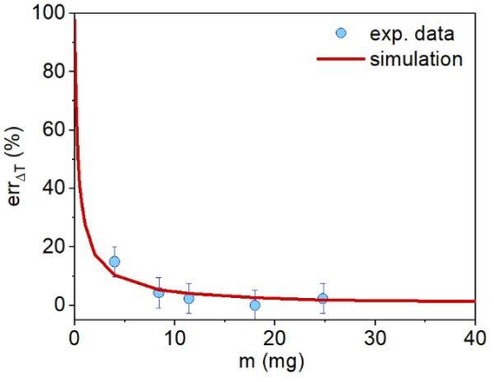

Figure 2 Experimental error, due to non-ideal adiabatic conditions, that affects the ΔT_{ad} measurement of a Gd thin sheet as a function of its progressively reduced mass (details on the experiment: Ref. 18).

4 Temperature sensor

4.1 Thermal mass

The second issue that needs to be considered concerns the temperature sensor and the thermal contact between it and the sample. Standard temperature sensors (thermocouples and resistive sensors) are electric transducers that require the achievement of the thermal equilibrium with the sample through heat exchange. The sample-sensor heat exchange, that is essential to

perform the temperature measurement, breaks the adiabatic condition of the sample. The amount of heat that flows between sample and sensor is ruled by the sensor heat capacity and it can significantly affect the measured value of ΔT_{ad}. By considering zero the heat losses to the surroundings ($K_{s\text{-}e}$ and $K_{t\text{-}e}$ = 0), the equilibrium temperature between sensor and sample (T_{eq}) results from the balancing of their thermal capacities, as can be derived from the calculation of charge distribution between C_s and C_t of the equivalent electrical circuit (Figure 1.b). By considering the same initial temperature (T_0) for sample and sensor and a ΔT_{ad} of the sample, the value of the temperature change that is measured by the sensor (ΔT_{ad}^*) is:

$$\Delta T_{ad}{}^{*} = \Delta T_{ad} \frac{C_s}{C_s + C_t} \qquad (2)$$

Equation 2 was experimentally demonstrated in Ref. 17 by measuring different masses of the same MC sample. To get a correct measurement of ΔT_{ad}, the ratio between the heat capacities of sensor and sample must tend to zero. Otherwise, it is important to make a post-measurement correction of the ΔT_{ad} values (equation 2), in order to take into account the heat exchanged with the temperature sensor.

This issue becomes particularly important in the case of samples with a small thermal mass. The previous paragraph already discussed the effect of non-ideal adiabatic conditions on the ΔT_{ad} that is measured on samples with a small mass. However, the crucial aspect of this type of measurement is the temperature sensor, because of the very small thermal capacitance of the sample (Equation. 2). Very small thermocouples usually offer a suitable thermal mass, but their spherical shape reduces the sample-sensor thermal conductance. On the contrary, small thermoresistances promote a good conductance at the interface but normally have a too large thermal mass. A proposed solution is to measure stacks of samples, [33] however in this case it is difficult to discriminate possible effects due to inhomogeneities of the samples or to the contribution of thermal paste that is used between the sheets. Non-contact techniques for the measurement of temperature were also proposed: they offer a clear advantage in terms of adiabatic conditions due to the elimination of a massive sensor in contact with the sample that unavoidably acts as a heat absorber. Thermo-acoustic methods [21,22,34] and setups based on the detection of the IR thermal radiation [18,23,24,35] have been developed. They were successfully utilized to measure the ΔT_{ad} of micrometric ribbons [34,35] and, in one case, of a thin film. [24] However, these experimental setups usually exploit a small alternate magnetic field (up to tens of mT). The direct test of MC response to magnetic stimuli actually used in technological applications is not achieved. Only two publications report the measurement performed on a single micrometric ribbon with a magnetic field change of 1 T. [18,25] In the first, the ΔT_{ad} measurement of a Gd micrometric sheet, was achieved thanks to the combination of a thermopile, a non-contact temperature sensor that measures the emitted thermal radiation, and a special designed sample holder made of a nylon frame inside a thermally controlled case. [18] Instead, the second paper reports measurements performed on micrometric Heusler ribbons, obtained by exploiting a thermo-optical effect and a pulsed magnetic field. [25] However, also these instruments are limited by the sample thickness, due to the heat dissipated during the measurement. [18] An experimental setup that is able to directly measure the MCE of very thin samples induced by a magnetic field change at least of 1 T, by combining a non-contact temperature sensor and a fast field change, has not be developed until now.

4.2 Response time

Another important parameter of the temperature sensor is its response time. By considering the sample as an infinite thermal source ($C_s >> C_t$) at the temperature T_s, the characteristic measurement time (or measurement time constant, τ_m), required for the sensor to reach 63% of sample temperature, depends on the sensor heat capacity and on the thermal conductance of the sensor-sample interface (K_{s-t}), which is the product of the coefficient of thermal contact conductance with the contact surface area ($K_{s-t} = k_{s-t} \cdot A$): [36]

$$\tau_m = \frac{C_t}{K_{s-t}} \tag{3}$$

If we consider a temperature difference ΔT between sample and sensor, the time profile of temperature measured by the sensor follows the function:

$$T_t(t) = T_0 + \Delta T_{ad}(1 - e^{-\frac{t}{\tau_m}}) \tag{4}$$

Equations 3 and 4 are obtained by solving the heat equation of the sample-sensor system or the equivalent electrical circuit with $C_s >> C_t$ and $R_{s-t} = K_{s-t}^{-1}$. This asymptotic growth function shows that an infinite time is required to reach the thermal equilibrium between sample and sensor. However, in real measurements, the temperature is considered stable when a quasi-equilibrium state is reached. This state is defined by the finite accuracy requested in the measurement of temperature.

This behaviour is more complex in the case of direct ΔT_{ad} measurements, because the temperature of the sample is not constant, but it changes due to the magnetic field variation. Generally, the time dependence of the temperature, that is recorded during a ΔT_{ad} measurement, is a convolution of: (a) the time profile of the external magnetic field $\Delta H(t)$, (b) the magnetic field dependence of the MCE $\Delta T_{ad}(\Delta H)$ and (c) the response function of the temperature sensor $T_t(\Delta T_{ad})$.

$$T_t(t) = T_t(\Delta T_{ad}) * \Delta T_{ad}(\Delta H) * \Delta H(t) \tag{5}$$

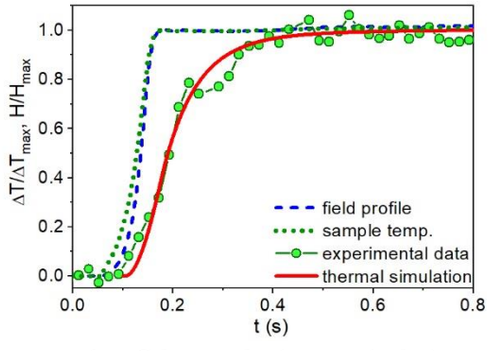

Figure 3: direct ΔT_{ad} measurement of a Gd sample (green circles) compared with: the corresponding magnetic field variation (blue dashed line), the expected temperature variation of the sample (green dotted line) and the outcome of a heat transfer simulation (red continuous line).

Figure 3 reports an example of ΔT_{ad} measurement performed on a Gd sample by rapidly inserting the sample inside a static magnetic field. [17] The green circles represent the experimental data, normalized to the maximum ΔT_{ad}. The measured time profile of the ΔT_{ad} is compared to the time profile of the magnetic field change (blue dashed line), that was measured with a pickup coil placed near the sample. The magnetic field takes about 70 ms to sweep through the 90% of its full change. A time delay between the field profile and the measured temperature change is evident and cannot be explained with the magnetic field dependence of the MCE across a second-order transition ($\Delta T_{ad} \propto H^{2/3}$, [37] shown by the dotted line). Instead, this delay results from the convolution of the magnetic field time profile with the time response of the temperature sensor. The outcome of a finite-difference heat transfer simulation of the thermodynamic system is shown with the continuous red line. The simulation matches well with the experimental data. From these results, we obtain a minimum characteristic time for this specific experimental setup of 110 ms, which derives from the convolution of the magnetic field evolution in time (rising time of about 70 ms) and of the temperature sensor response function (characterized by a time constant of about 70 ms). This result is based on standard thermodynamic considerations and can be generalized to other instruments. The response time of the temperature sensor limits the time-resolution obtainable in a ΔT_{ad} measurement and, consequently, the evaluation of the filed dependence of the adiabatic temperature change ($\Delta T_{ad}(\Delta H)$) derived from $\Delta T_{ad}(t)$ measurements.

Besides the thermal features of temperature sensor, also the thermal contact between it and the sample plays an important role to define the characteristic time of ΔT_{ad} measurement and to establish its accuracy (Equation 3). The quality of thermal contact depends on the characteristics of the sample surface, on the extension of contact area and on the features and thickness of the conductive paste laid between sample and sensor. A poor thermal contact between sample and sensor increases the time required to complete the temperature measurement and, thus, the dissipated heat from the sample. Achieving a good thermal contact can be difficult especially with a small temperature sensor and with porous or rough samples. The use of a conductive paste improves the thermal contact, but it introduces a further source of heat loss, because the paste acts as an additional thermal mass that absorbs heat from the sample.

Figure 4 shows the outcomes of finite-difference thermal simulations performed on the schematized system reported in Figure 1.a, by considering 4 different values of the thermal contact conductance at the sensor-sample interface ($k_{s\text{-}t}$ = 1000, 100, 10 and 5 $Wm^{-2}K^{-1}$). The dashed line of Figure 4.a represents the magnetic field variation that was used in the simulation. The ΔT_{ad}, induced in the sample was considered proportional to $\Delta H^{2/3}$. Figure 4.a reports the temperature change measured as a function of time for the 4 values of $k_{s\text{-}t}$. The temperature variation obtained by considering the two larger values of conductance follows the intrinsic temperature change of the sample. Instead, the worsening of the thermal conductance increases the time-delay between the field change and the temperature change due to the reduction of the heat transfer at the interface. This effect becomes more evident if the temperature variation is reported as a function of the magnetic field applied to the material (Figure 4.b). This apparent change of the field behaviour of the MCE is not intrinsic to the MC material but it is due to the effect of thermal conductance between sample and sensor.

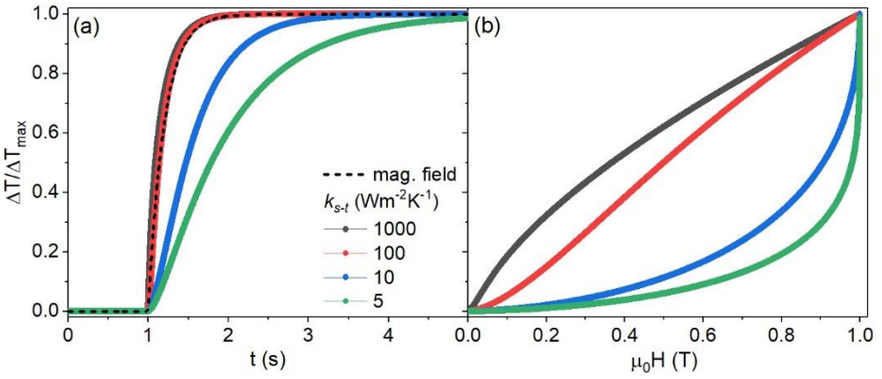

Figure 4: Outcomes of heat transfer simulations: ΔT_{ad} as a function of time (a) and of the applied magnetic field (b) by considering different values of the thermal contact conductance at the sensor-sample interface. The dashed line represents the magnetic field variation.

Similar results have been obtained experimentally. Figure 5 shows the adiabatic temperature change induced in a Gd sample by applying the same magnetic field change that was considered for the simulation. Four measurements have been obtained by inserting between sample and sensor an increasing number (0, 1, 5, 10) of Kapton thin sheets (60μm). As in the case of simulation, the worsening of the thermal contact at the sample-sensor interface increases the time requested for the heat-transfer and, consequently, to reach the maximum ΔT_{ad}. Moreover, due to the non-perfect adiabatic condition and to the non-negligible thermal mass of Kapton sheets, heat is dissipated during the measurement, thus decreasing the maximum adiabatic temperature change that is measured. Although the reported results represent an extreme case, they are useful to directly observe the non-negligible effect that interface thermal conductance has on the measured MCE, especially if its field dependence is calculated from measurements performed in the time domain.

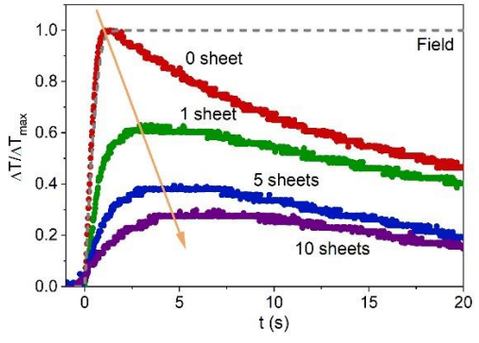

Figure 5: Direct ΔT_{ad} measurements of a Gd sample performed by inserting between the sample and the sensor an increasing number of insulating thin sheets.

The response time of the temperature sensor takes a very critical role in the case of measurements performed with fast field changes. Different experimental setups for the direct measurement of the MCE induced by pulsed magnetic fields were proposed in the literature. [8,9,11,19,20] The majority of them use very small thermocouples to detect the temperature variations of the sample. [8,9,11] However, though their response time is shorter if compared to other standard temperature sensors, it depends on many factors (the thermal mass of the junction, the quality of the contact with the sample and the heat dissipated trough the metallic wires) and cannot be easily controlled, thus introducing a variable effect in the measurement. An alternative solution,

consisting of a thin-film resistive thermometer directly grown on the sample surface, was proposed by Kihara et al. [19] This method ensures a prompt response time of the temperature sensor, but it requires a complex preparation of the sample that is not easily reproducible with porous or irregular samples. Alternatively, Cugini et al. proposed a method based on the thermo-optical "mirage effect". [20,25] This experimental setup measures the ΔT_{ad} by the deflection of a laser beam grazing to the sample surface due to the thermal gradient that develops in the air layer overlying the sample surface. This method was tested for the measurement of the MCE with a pulsed magnetic field of 1 T of bulk and ribbon samples showing both a second order and a first order magnetic transition. However, also for this method, the time required to stabilize the thermal exchange of the sample (on the order of tenths of milliseconds) limits the response time of the temperature change evaluation.

For all the presented experimental solutions, the prompt temperature acquisition is the crucial aspect to obtain the proper evaluation of the adiabatic temperature change. If the response time is larger or comparable with the characteristic time of the field change, it introduces a delay in the temperature measurement that affects the final estimation of ΔT_{ad} and the evaluation of possible intrinsic kinetic effects of the transitions. Moreover, the characteristic profile of magnetic field pulses causes a reduction of the maximum measurable ΔT_{ad} in the case of a delay between the temperature and magnetic field change. Indeed, the sign change of the time derivative of the magnetic field induces two opposite MCE. If the temperature sensor is not fast enough, a time-average of two opposite MCE is obtained, with a reduction of the maximum measured ΔT_{ad}.

Finite-difference heat transfer simulations were performed to the aim of directly observing this effect. We considered, as a model material, a Mn_3GaC sample, which undergoes both a very sharp first-order magnetic transition at about 150 K, with associated an inverse MCE, and a second-order Curie transition at about 250 K. [38,39] Adiabatic temperature change measurements of this sample, performed with a pulsed magnetic field, are reported in Ref. 38. The thermal system, schematized in Figure 1.a, was simplified by assuming perfect adiabatic condition ($K_{t\text{-}e}$ and $K_{s\text{-}e} = 0$) and the sample thermal capacitance much larger than that of the sensor ($C_s >> C_t$). A spherical chromel-constantan thermocouple, of radius r, specific heat c_t and density ρ, was considered placed inside the sample. The contact area between sample and sensor was approximated as the full sensor surface $A = 4\pi r^2$. The thermal contact conductance was assumed very good, with a coefficient ($\alpha = 100$ kW m^{-2} K^{-1}) lying within the range of values reported in literature for a thermal contact between two pressed solid surfaces. [40] The magnetic field pulse, that was used for the simulation, has an amplitude of 10 T and a rise time of about 1 ms (Figure 6.b, dashed line). Simulations were carried out by considering both the Curie transition (T = 258 K) and the first-order transition (T = 150 K) of the material. Figure 6.a reports the field dependences of the ΔT_{ad} that were utilized in the two cases. For the Curie transition, ΔT_{ad} follows the $H^{2/3}$ behaviour (red line in the upper part of Figure 6.a). According to Ref. [38], a maximum ΔT_{ad} of 2 K was considered for a $\mu_0 \Delta H = 10$ T at 258 K. In the case of the first-order transition, we considered ΔT_{ad} occurring in a field interval of about 0.3 T (ΔH_{trans}) starting from a critical field: $H_{c1} = 2.6$ T by increasing the field and $H_{c2} = 1.4$ T by decreasing the field. [38] Outside from these field intervals the sample temperature does not change. The effect of the direct MCE, superimposed to the inverse MCE due to the first-order transition, is neglected. The maximum considered ΔT_{ad} is 4 K. [38]

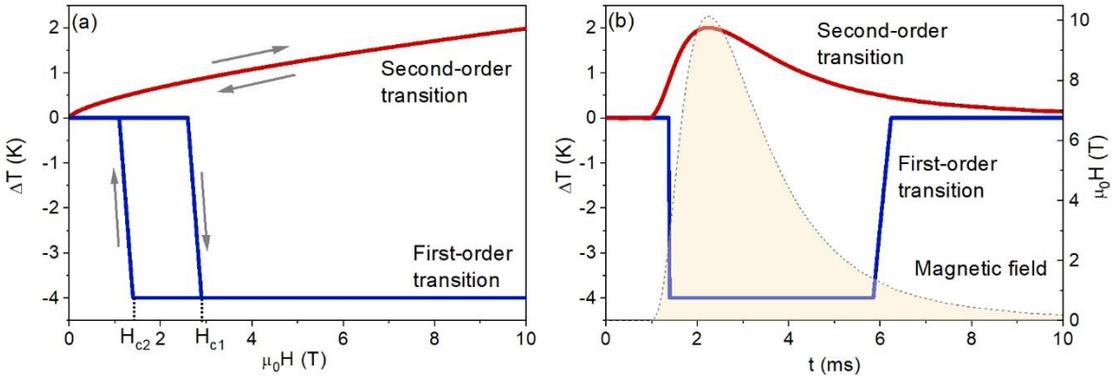

Figure 6 (a) Sample temperature change as a function of the applied magnetic field for the second-order (red line) and the first-order (blue line) magnetic transition. (b) Time profile of the sample temperature change at the second-order (red line) and the first-order (blue line) magnetic transition induced by a pulsed magnetic field (dashed line).

The simulation was repeated by using different radii of the temperature sensor (1.0, 4.0 and 10.0 μm). This allows to simulate different conditions in the adiabatic temperature change measurement. Indeed, if we consider Equation 3 for the specific system of the simulation, we obtain that the characteristic time constant of the temperature sensor is ruled by its specific heat, its density, its radius and the coefficient of thermal contact conductance at the interface ($k_{s\text{-}t}$):

$$\tau = \frac{c_s \rho}{3k_{s-t}} r \qquad (6)$$

By increasing the radius of the thermocouple, we are simulating an increase of its thermal capacitance or a worsening of the thermal contact between it and the sample.
The outcomes of simulation are reported as a function of time in Figure 7.a and as a function of the applied magnetic field in Figure 7.b. The variation of the intrinsic temperature of the sample is reported with the dashed lines. In the case of the MCE at the Curie temperature (on the top of the Figure 7.a), we do not observe a pronounced difference between the outcomes of the three temperature sensors and the intrinsic temperature of the sample. On the contrary, in the case of the first-order transition (on the bottom), we appreciate a delay in the measured $\Delta T(t)$ that increases by increasing the radius of the sensor. This difference becomes more evident if we plot the temperature change as a function of the applied magnetic field (Figure 7.b). At the Curie temperature we observe a lenticular shape of the $\Delta T(H)$ curve for the biggest sensor (red line on the top of Figure 7.b), while the other two sensors show a small delay with respect to the intrinsic temperature of the sample (dashed line). On the contrary, in the case of the first-order transition the very strong field-dependence of temperature change brings to a time delay for the temperature measured by all the sensors, which increases with the radius. We observe also that in the decreasing part of the field pulse the delay is less marked due to the lower field sweep rate.

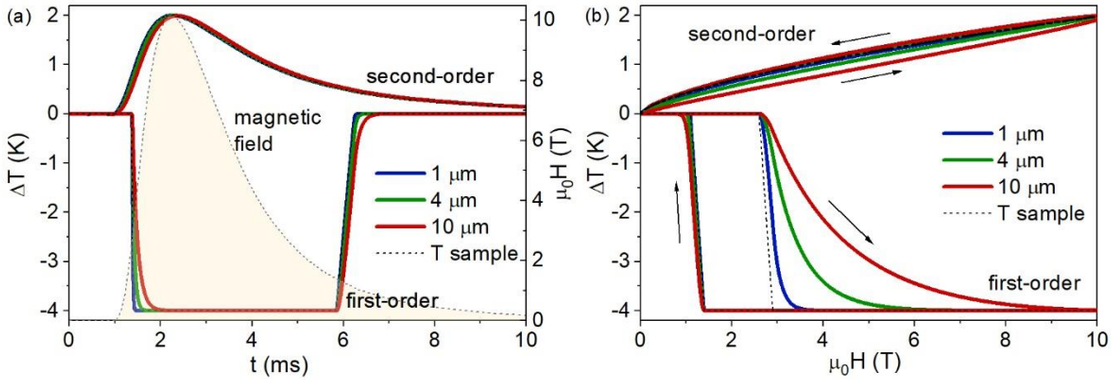

Figure 7 Outcomes of finite-difference simulation. (a) Temperature change of Mn_3GaC induced by a pulsed magnetic field (dashed line) at the second-order (on the top) and first-order (on the bottom) magnetic transition. The temperature variation is measured by considering 3 different sensors with a radius of 1, 4 and 10 μm. (b) Measured temperature change as a function of the applied magnetic field. Dashed line: variation of the intrinsic temperature of the sample.

These results confirm the crucial role of the temperature sensor and of the sensor-sample thermal interface in determining the time scale at which the ΔT_{ad} measurements are reliable. Indeed, if the response time of the experimental setup is comparable to the characteristic time of the field change, it is not possible to reliably discriminate between the effect of the sensor and a possible time lag due to the intrinsic kinetics of transformation. This can bring to an ambiguous interpretation of results.

5 Material properties

5.1 Thermal conductivity

All the discussions of the previous paragraphs considered the sample as a single body in which the MCE develops and that exchanges heat with the temperature sensor and with the surroundings. Indeed, also the thermodynamic properties of the sample can affect the ΔT_{ad} measurement. In particular, the sample thermal conductivity can modify the time profile of the measured ΔT_{ad}. Porcari et al. and Sellschopp et al. experimentally demonstrated that the sample thermal conductivity can drastically influence the measurement of the dynamic response of magnetocaloric materials [41,42]. Their results can be understood by considering the simplified sketch of Figure 8: the magnetocaloric sample can be schematized as a stack of several (infinite) sections in which the MCE develops and that exchange heat with the adjacent layers. Only the section in contact with the sensor directly exchanges heat with it. The heat transferred from the other layers crosses the material in order to reach the temperature sensor. This requires a finite time interval.

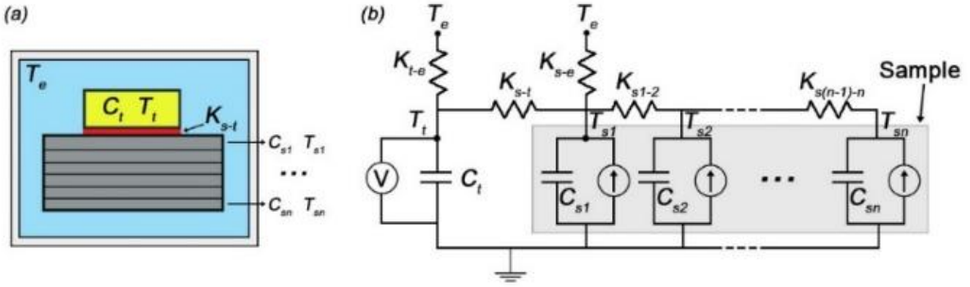

Figure 8 Schematic illustration (a) and equivalent electrical circuit (b) of the experimental system to directly measure the adiabatic temperature change, by considering the effect of the material thermal conductivity.

In the electrical equivalent circuit, the sample is approximated as a series of capacitances and current sources, connected in parallel (Figure 8.b). The heat transfer among the sections is ruled by the effective thermal conductivity (K_s) of the material, which includes also possible extrinsic factors such as the presence of inter-grains thermal resistances [42]. This results in a correlation between the material thermal conductivity and the characteristic time constant τ_m of a ΔT_a measurement. Therefore, Equation 3 can be expanded as:

$$\tau_m \approx C_t \left(\frac{1}{K_{s-t}} + \frac{1}{gK_s}\right) \qquad (7)$$

The above result was obtained by solving the electrical circuit, neglecting the heat dissipations to the environment and considering an overall effect of material thermal conductivity K_s, corrected by a factor g, which takes into account the geometrical features of the sample. Equation 7 clearly shows that poor thermal properties of the material can alter the measurement of the adiabatic temperature change, by introducing a time delay between the field and the temperature change. This was experimentally verified in Ref. [41].
A similar model was utilized by Kuz'min in Ref. [43] to evaluate the time required for the heat exchange between a layered MC bed and a heat exchanger of a refrigerator. The equation 6 of Ref. [43] highlights, similarly to equation 7 of this manuscript, the significant role of the material thermal conductivity in determining the characteristic time of heat transfer driven by the MCE and, consequently, the maximum operating frequency of magnetic refrigerator.

5.2 Irreversibility of first-order transitions

Besides the characteristics of the experimental setup, also the measurement protocol can produce different ΔT_{ad} results in the case of first-order magnetic transitions [44,45]. This issue is related to the irreversibility, characteristic of first-order transitions, and to the broadening of real transitions that allows partial transformations between mixed states [46–48]. The state of a material, in the hysteresis region, is not univocally defined by the thermodynamic variables (magnetic field and temperature) but depends on its thermo-magnetic history. Consequently, also the ΔT_{ad} associated to a partial transition between two mixed states strongly depends on the thermomagnetic history of the sample.
Caron et al. discussed the effect of different protocols on the calculation of the isothermal entropy change from magnetization measurements. [49] In the case of ΔT_{ad}, the risk of

overestimating the MCE is avoided, because of the direct nature of the measurement. However, the use of different measurement protocols results in distinct information. In a schematized view, two main protocols can be used to perform adiabatic temperature change measurements: (1) a "phase-reset protocol" and (2) a "cyclic protocol".

The "phase-reset protocol" results in the maximum ΔT_{ad} that can be obtained for a ΔH field change at a specific temperature. It is useful to explore the intrinsic nature of a material, by measuring the maximum MCE that can be compared with the values derived from indirect techniques, such as magnetometry and in-field calorimetry. [50] This protocol is similar to that adopted for *M(H)* measurements used to calculate Δs_T. [49] It is based on the reset of a univocal starting phase of the material before to perform each ΔT_{ad} measurement. Figures 9 schematizes, in a field-temperature phase diagram, the protocol in the case of a direct (Figure 9.a) and an inverse (Figure 9.b) MCE. The continuous lines mark the two opposite transitions that occurs between the low-temperature (LT) and the high-temperature (HT) phase. Both the temperature and field hysteresis are present between the two lines. The dashed lines schematize the broadening on a finite temperature/field range of real first-order transitions. [46] The difference between the two cases (Figure 9.a and Figure 9.b) is due to the opposite dependence of the critical temperature to the magnetic field (dT_c/dH), that is positive for the direct MCE and negative for the inverse MCE. This is due to the different change in the magnetization by moving from the LT to the HT phase (dM/dT): the direct MCE is related to a transition from a large magnetization to a low magnetization phase ($dM/dT > 0$), the inverse MCE is due to the opposite case ($dM/dT < 0$). For simplicity we refer, in the following, to "direct transition" for the first case and "inverse transition" for the second. The opposite field-dependence of the critical temperature makes necessary the use of two opposite protocols in order to avoid hysteretic effects. In the case of the direct transition (Figure 9.a, green arrows on the bottom) the material has to be heated up, before each ΔT_{ad} measurement, in order to reset the HT phase. The broadening of the transition defines the temperature that has to be overcome to ensure a complete transition to the HT phase. After that, the sample is cooled down to the desired temperature in zero applied field, and the ΔT_{ad} measurement is performed by applying the field. The ΔT_{ad} is due to the field-induced transformation from the HT to the LT phase. Since that mixed metastable states near the magnetic transition are, usually, very sensitive to temperature variations and fluctuations, a careful attention has to be paid to the temperature sweep used before to perform the measurement (e.g.: a fixed sweep rate is recommended, temperature overshooting and time delays has to be avoided…). [51]

Instead, if we want to measure the ΔT_{ad} related to the transition from the LT to the HT phase, the opposite protocol has to be followed: (1) the material is cooled down, in order to reset the LT phase, (2) the magnetic field is applied, (3) the temperature of the sample is increased by maintaining applied the magnetic field, (4) the ΔT_{ad} is measured by removing the field (upper violet arrows in Figure 9.a).

In the case of inverse first-order transitions the opposite protocol has to be used: (1) reset the LT phase, (2) heating the sample in zero applied field and (3) measure the ΔT_{ad} by applying the field (green arrows on the bottom, Figure 9.b). Otherwise: (1) stabilize the HT phase, (2) cool down the sample under the applied field and (3) measure the ΔT_{ad} by removing the field (upper violet arrows, Figure 9.b).

The field-dependence of the critical temperature univocally determine the protocol that must be used to completely measure the MCE on the first shot. An example can be found in Ref. [45]: the authors report ΔT_{ad} measurements performed by following different "discontinuous protocols"

on a material showing an inverse first-order transition. In all their measurements the sample temperature was changed in zero applied magnetic field and the ΔT_{ad} was detected by increasing the field. They found that the results obtained stabilizing the LT phase are higher than that measured by starting from the HT phase. This is understandable by looking at Figure 9.b. In the first case, they followed the protocol sketched in the Figure with the green arrows on the bottom: the LT phase is stabilized and the measured ΔT_{ad} is the result of the LT→HT transformation, induced by the application of the magnetic field. Instead, when the field is applied to the material stabilized in the HT phase a lower MCE occurs. This because an increase of the field always induces, for inverse transitions, a LT→HT transformation. The resulting MCE is only related to the fraction of LT phase that has been transformed by cooling the material before to perform the ΔT_{ad} measurement. Due to the thermal hysteresis this fraction is lower than the fraction of LT obtained by heating the material at the same temperature by starting from a complete LT phase.

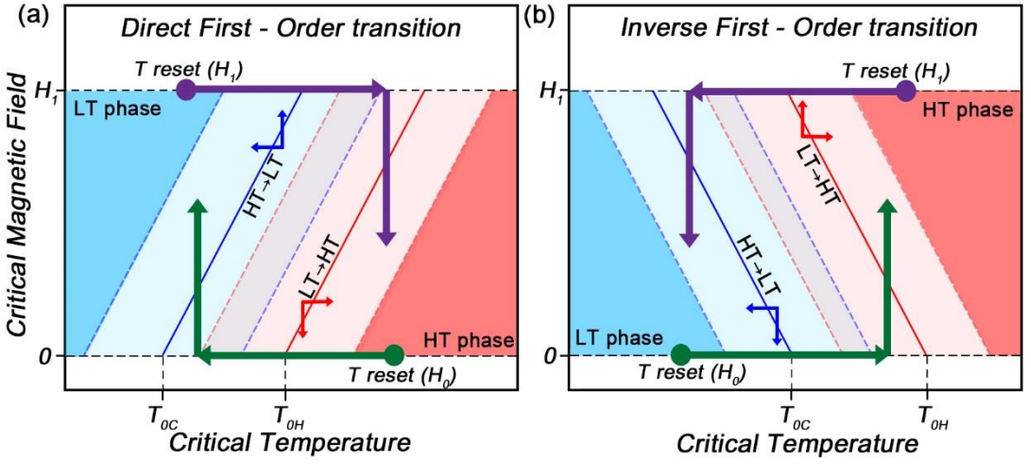

Figure 9 Schematic illustration of the "phase-reset protocol" for the measurement of the ΔT_{ad} in the case of a "direct" (a) or an "inverse" (b) first-order transition.

Unlike measurements performed with the "phase-reset" protocol, the "cyclic protocol" allows the direct measurement of the reversible ΔT_{ad} that can be exploited in thermo-magnetic cycles [6,17,48]. This protocol consists in the continuous measurement of the ΔT_{ad} with a cyclical application of the magnetic field to the material while the temperature of the environment is maintained constant or is slowly sweeped. Only the reversible part of the ΔT_{ad} is measured. This protocol can be indistinctly applied on heating or on cooling for both second-order and first order transitions. However, due to the hysteresis of first order transitions, different temperature behaviour of ΔT_{ad} are expected by performing the measurement on cooling or on heating. [52] Moreover, the sweep rate and the frequency of the field change can bring to different results due to the transformation between mixed states. [44]

Figure 10 reports, as a case of study, a comparison of ΔT_{ad} values of a $Ni_{49.6}Mn_{34.2}In_{16.1}$ sample measured by following both the "phase-reset protocol" and the "cyclic protocol". The sample belongs to the Heusler family of compounds and shows an inverse first-order magnetostructural transition (T_t = 301.5 K on heating in zero applied magnetic field) near the Curie transition (T_c = 309 K) of the HT ferromagnetic phase. [53] The yellow circles, in Figure 10.a, are the ΔT_{ad} values derived from the measurement performed by following the "cyclic protocol". Both the direct MCE

at the second-order transition (T_C = 309.0 K) and the inverse MCE, with a maximum at about 295 K, are shown. The measurement was performed by cyclically turning on and off a 1.8 T magnetic field with a period of 30 s, during a temperature sweep on cooling (sweep rate: 0.5 $Kmin^{-1}$). A portion of the measurement is reported in Figure 10.b. The ΔT_{ad} values reported in the Figure 10.a correspond to the MCE induced by switching off the field. Instead, the squares and the triangles refer to the ΔT_{ad} calculated from single measurements performed with the "phase-reset protocol" on cooling (violet arrows of Figure 9.b). Before each measurement, the sample was heated up to 310 K and cooled to the desired temperature by maintaining the magnetic field (1.8 T) applied. Then the magnetic field was subsequently removed and applied for three times. An example of measurement at 295 K is reported in Figure 10.c. The reduction of the measured ΔT_{ad} for the second field variation is evident. The results of measurements performed at different temperatures are summarized in Figure 10.a: the squares are the ΔT_{ad} induced by the first turning off of the field, the triangles report the ΔT_{ad} measured for the second decrease of the field. In the case of the second-order transition, near 308 K, both the protocols result in the same ΔT_{ad} values. Instead, for the first-order transition the ΔT_{ad} obtained with the first change of the magnetic field in the "phase-reset protocol" results significantly larger than that induced by the second removal of the field or by using the "cyclic protocol". Whereas, the ΔT_{ad} induced by the second field change is consistent with the value obtained with the "cyclic protocol".

These results are used as an example to probe the dependence of the measured ΔT_{ad} on the thermo-magnetic history of the sample in the case of first-order transitions. This implies that ΔT_{ad} measurements should be always accompanied by a detailed description of the experimental protocol that is used. This allows the comparison of different results and materials.

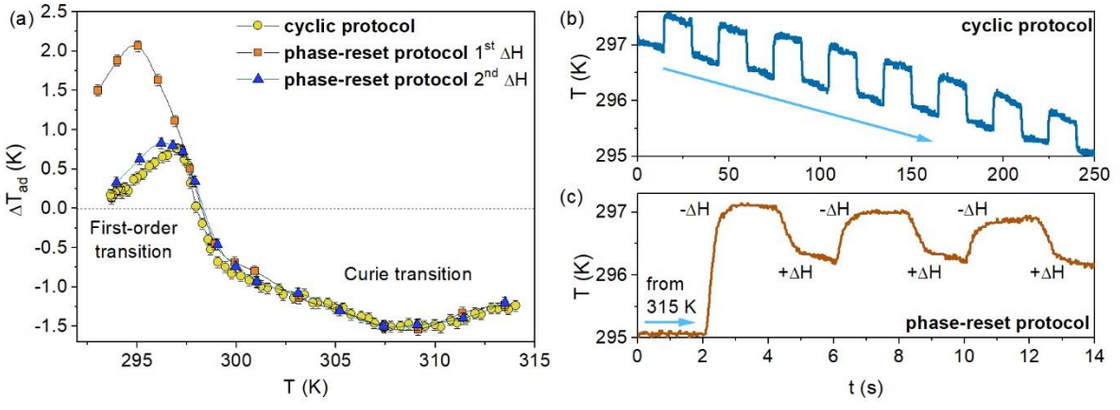

Figure 10 (a) $\Delta T_{ad}(T)$ of $Ni_{49.6}Mn_{34.2}In_{16.1}$ sample measured by following the "phase-reset protocol" (squares and triangles) and the "cyclic protocol" (circles) on cooling with a magnetic field change of 1.8 T. (b) Part of the measurement performed with the "cyclic protocol" on cooling. (c) Example of a measurement at 295 K with the "phase-reset protocol".

6 Conclusions

In conclusion, we discussed the main issues that can affect a direct adiabatic temperature change measurement of a magnetocaloric material. Finite-difference thermal simulations and special designed experiments demonstrated the non-negligible role of non-ideal adiabatic conditions and of the temperature sensor in determining the maximum value and the field

dependence of the measured adiabatic temperature change. In particular, the quality of adiabatic conditions and the thermal mass of the temperature sensor are critical to correctly measure the temperature change of small samples. Whereas, the response time of the temperature sensor plays a significant role in the determination of the MCE induced by fast field changes. Finally, the effect of different measurement protocols has been analysed by measuring, as a case of study, a NiMnIn Heusler compound, showing both a second-order and a first-order magnetic transition. This work offers a practical guide for the design of an experimental setup aimed at directly measuring the adiabatic temperature change of magnetocaloric materials and at analysing and interpreting the experimental results, in order to clearly separate the intrinsic effect of the material from the contribution of experimental configuration. Moreover, the results and conclusions of this work are extendable to the measurement of other caloric effects induced by a different stimulus (electrical or mechanical).

Acknowledgment

The authors acknowledge: G. Porcari, who significantly contributed to start this research; Ö. Çakır (Yildiz Technical University, Turkey), F. Scheibel (TU Darmstad, Germany) and R. Cabassi (IMEM-CNR Institute, Parma, Italy) for useful discussions; C. Bennati, S. Fabbrici and F. Albertini (IMEM-CNR Institute, Parma, Italy) for the Heusler sample.

References

[1] P. Spoonley, Int. J. Refrig. **24**, 593 (2001).
[2] A. Kitanovski, J. Tušek, U. Tomc, U. Plaznik, M. Ožbolt, and A. Poredoš, *Magnetocaloric Energy Conversion From Theory to Applications* (Springer, 2015).
[3] A.M. Tishin and Y.I. Spichkin, *The Magnetocaloric Effect and Its Applications* (IOP Publishing, 2003).
[4] T. Gottschall, K.P. Skokov, M. Fries, A. Taubel, I. Radulov, F. Scheibel, D. Benke, S. Riegg, and O. Gutfleisch, Adv. Energy Mater. Mater. **34**, 1901322 (2019).
[5] K. Morrison, K.G. Sandeman, L.F. Cohen, C.P. Sasso, V. Basso, A. Barcza, M. Katter, J.D. Moore, K.P. Skokov, and O. Gutfleisch, Int. J. Refrig. **35**, 1528 (2012).
[6] F. Guillou, G. Porcari, H. Yibole, N. Van Dijk, and E. Brück, Adv. Mater. **26**, 2671 (2014).
[7] B. Yu, M. Liu, P.W. Egolf, and A. Kitanovski, Int. J. Refrig. **33**, 1029 (2010).
[8] S.Y. Dan'kov, A.M. Tishin, V.K. Pecharsky, and K.A. Gschneidner, Rev. Sci. Instrum. **68**, 2432 (1997).
[9] J. Kamarád, J. Kaštil, and Z. Arnold, Rev. Sci. Instrum. **83**, 083902 (2012).
[10] X. Moya, L. Mañosa, A. Planes, S. Aksoy, M. Acet, E.F. Wassermann, and T. Krenke, Phys. Rev. B **75**, 184412 (2007).
[11] M. Ghorbani Zavareh, C. Salazar Mejía, A.K. Nayak, Y. Skourski, J. Wosnitza, C. Felser, and M. Nicklas, Appl. Phys. Lett. **106**, 071904 (2015).
[12] K.P. Skokov, V. V. Khovaylo, K.H. Müller, J.D. Moore, J. Liu, and O. Gutfleisch, J. Appl. Phys. **111**, 07A910 (2012).
[13] S.M. Benford and G. V. Brown, J. Appl. Phys. **52**, 2110 (1981).
[14] F. Canepa, S. Cirafici, M. Napoletano, C. Ciccarelli, and C. Belfortini, Solid State Commun. **133**, 241 (2005).
[15] A.M. Aliev, A.B. Batdalov, L.N. Khanov, V. V. Koledov, V.G. Shavrov, I.S. Tereshina, and S. V. Taskaev, J. Alloys Compd. **676**, 601 (2016).
[16] B.R. Gopal, R. Chahine, and T.K. Bose, Rev. Sci. Instrum. **68**, 1818 (1997).

[17] G. Porcari, M. Buzzi, F. Cugini, R. Pellicelli, C. Pernechele, L. Caron, E. Brück, and M. Solzi, Rev. Sci. Instrum. **84**, 073907 (2013).
[18] F. Cugini, G. Porcari, and M. Solzi, Rev. Sci. Instrum. **85**, 074902 (2014).
[19] T. Kihara, Y. Kohama, Y. Hashimoto, S. Katsumoto, and M. Tokunaga, Rev. Sci. Instrum. **84**, 074901 (2013).
[20] F. Cugini, G. Porcari, C. Viappiani, L. Caron, A.O. Dos Santos, L.P. Cardoso, E.C. Passamani, J.R.C. Proveti, S. Gama, E. Brück, and M. Solzi, Appl. Phys. Lett. **108**, 012407 (2016).
[21] B.R. Gopal, R. Chahine, M. Földeàki, and T.K. Bose, Rev. Sci. Instrum. **66**, 232 (1995).
[22] A.O. Guimarães, M.E. Soffner, A.M. Mansanares, A.A. Coelho, A. Magnus, G. Carvalho, M.J.M. Pires, S. Gama, and E.C. da Silva, Phys. Rev. B **80**, 134406 (2009).
[23] D. V. Christensen, R. Bjørk, K.K. Nielsen, C.R.H. Bahl, A. Smith, and S. Clausen, J. Appl. Phys. **108**, 063913 (2010).
[24] J. Döntgen, J. Rudolph, T. Gottschall, O. Gutfleisch, S. Salomon, A. Ludwig, and D. Hägele, Appl. Phys. Lett. **106**, 032408 (2015).
[25] F. Cugini, D. Orsi, E. Brück, and M. Solzi, Appl. Phys. Lett. **113**, 232405 (2018).
[26] A. Kitanovski and P.W. Egolf, Int. J. Refrig. **33**, 449 (2010).
[27] D.J. Silva, B.D. Bordalo, A.M. Pereira, J. Ventura, and J.P. Araújo, Appl. Energy **93**, 570 (2012).
[28] S. V. Taskaev, M.D. Kuz'Min, K.P. Skokov, D.Y. Karpenkov, A.P. Pellenen, V.D. Buchelnikov, and O. Gutfleisch, J. Magn. Magn. Mater. **331**, 33 (2013).
[29] S. Taskaev, K. Skokov, D. Karpenkov, V. Khovaylo, M. Ulyanov, D. Bataev, A. Pellenen, A. Fazlitdinova, and O. Gutfleisch, J. Magn. Magn. Mater. 6 (2017).
[30] F. Cugini, L. Righi, L. van Eijck, E. Brück, and M. Solzi, J. Alloys Compd. **749**, 211 (2018).
[31] F. Puglielli, V. Mussi, F. Cugini, N. Sarzi Amadè, M. Solzi, C. Bennati, S. Fabbrici, and F. Albertini, Front. Energy Res. **7**, 150 (2020).
[32] V. Basso, C.P. Sasso, and M. Küpferling, Rev. Sci. Instrum. **81**, 1 (2010).
[33] A. Waske, H. Hermann, N. Mattern, K. Skokov, O. Gutfleisch, and J. Eckert, J. Appl. Phys. **112**, 123918 (2012).
[34] A.M. Mansanares, F.C.G. Gandra, M.E. Soffner, A.O. Guimarães, E.C. Da Silva, H. Vargas, and E. Marin, J. Appl. Phys. **114**, 163905 (2013).
[35] J. Döntgen, J. Rudolph, A. Waske, and D. Hägele, Rev. Sci. Instrum. **89**, 033909 (2018).
[36] J. Fraden, *AIP Handbook of Modern Sensors: Physics, Designs, and Applications* (American Institute of Physics, 1993).
[37] M.D. Kuzmin, K.P. Skokov, D.Y. Karpenkov, J.D. Moore, M. Richter, and O. Gutfleisch, Appl. Phys. Lett. **99**, 012501 (2011).
[38] F. Scheibel, T. Gottschall, K. Skokov, O. Gutfleisch, M. Ghorbani-Zavareh, Y. Skourski, J. Wosnitza, Ö. Çakir, M. Farle, M. Acet, Ö. Çakır, M. Farle, and M. Acet, J. Appl. Phys. **117**, 233902 (2015).
[39] Ö. Çakir and M. Acet, Appl. Phys. Lett. **100**, 202404 (2012).
[40] K. Nishino, S. Yamashita, and K. Torii, Exp. Therm. Fluid Sci. **10**, 258 (1995).
[41] G. Porcari, K. Morrison, F. Cugini, J.A.A. Turcaud, F. Guillou, A. Berenov, N.H.H. Van Dijk, E.H.H. Brück, L.F.F. Cohen, and M. Solzi, Int. J. Refrig. **59**, 29 (2015).
[42] K. Sellschopp, B. Weise, M. Krautz, F. Cugini, M. Solzi, L. Helmich, A. Waske, A. Hütten, and A. Waske, Energy Technol. **6**, 1448 (2018).
[43] M.D. Kuz'min, Appl. Phys. Lett. **90**, 251916 (2007).
[44] L.M. Moreno-Ramírez, A. Delgado-Matarín, J.Y. Law, V. Franco, A. Conde, and A.K. Giri, Metals (Basel). **9**, 1144 (2019).
[45] C. Salazar-Mejía, V. Kumar, C. Felser, Y. Skourski, J. Wosnitza, and A.K. Nayak, Phys. Rev. Appl. **11**, 054006 (2019).
[46] F. Cugini, G. Porcari, S. Fabbrici, F. Albertini, and M. Solzi, Philos. Trans. R. Soc. A Math. Phys. Eng. Sci. **374**, 20150306 (2016).
[47] F. Cugini, G. Porcari, T. Rimoldi, D. Orsi, S. Fabbrici, F. Albertini, and M. Solzi, Jom **69**,

1422 (2017).
[48] T. Gottschall, K.P. Skokov, B. Frincu, and O. Gutfleisch, Appl. Phys. Lett. **106**, 021901 (2015).
[49] L. Caron, N. Ba Doan, and L. Ranno, J. Phys. Condens. Matter **29**, 075401 (2017).
[50] G. Porcari, F. Cugini, S. Fabbrici, C. Pernechele, F. Albertini, M. Buzzi, M. Mangia, and M. Solzi, Phys. Rev. B - Condens. Matter Mater. Phys. **86**, 104432 (2012).
[51] V. Basso, M. Piazzi, C. Bennati, and C. Curcio, Phys. Status Solidi Basic Res. **255**, 1 (2018).
[52] F. Guillou, H. Yibole, G. Porcari, L. Zhang, N.H. Van Dijk, and E. Brück, J. Appl. Phys. **116**, (2014).
[53] C. Bennati, S. Fabbrici, R. Cabassi, N.S. AMADè, F. Cugini, M. Solzi, and F. Albertini, in *Refrig. Sci. Technol.* (International Institute of Refrigeration, 2018), pp. 262–267.

AIP Publishing

Journal of Applied Physics

ACCEPTED MANUSCRIPT

This is the author's peer reviewed, accepted manuscript. However, the online version of record will be different from this version once it has been copyedited and typeset.
PLEASE CITE THIS ARTICLE AS DOI: 10.1063/5.0002870

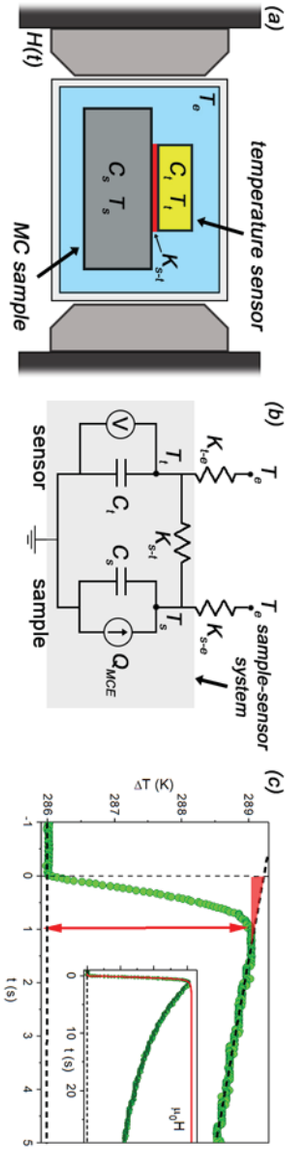

PLEASE CITE THIS ARTICLE AS DOI: 10.1063/5.0002870

AIP Publishing Journal of Applied Physics

PLEASE CITE THIS ARTICLE AS DOI: 10.1063/5.0002870

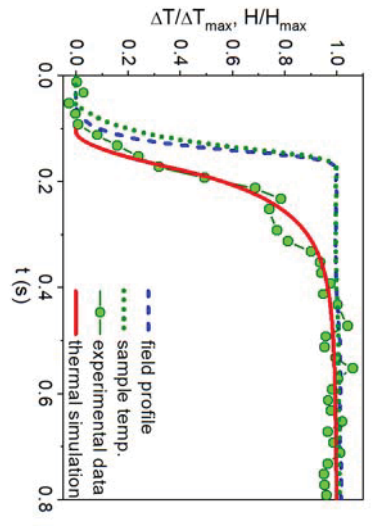

AIP Publishing
Journal of Applied Physics
ACCEPTED MANUSCRIPT

PLEASE CITE THIS ARTICLE AS DOI: 10.1063/5.0002870

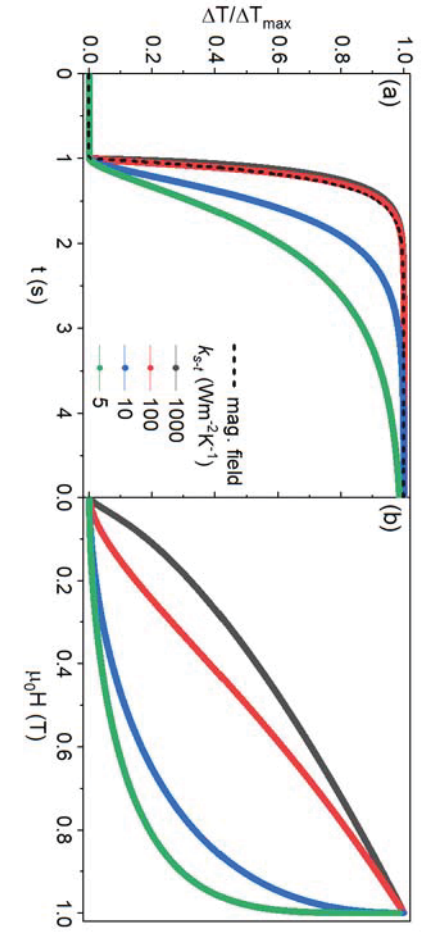

AIP Publishing Journal of Applied Physics

PLEASE CITE THIS ARTICLE AS DOI: 10.1063/5.0002870

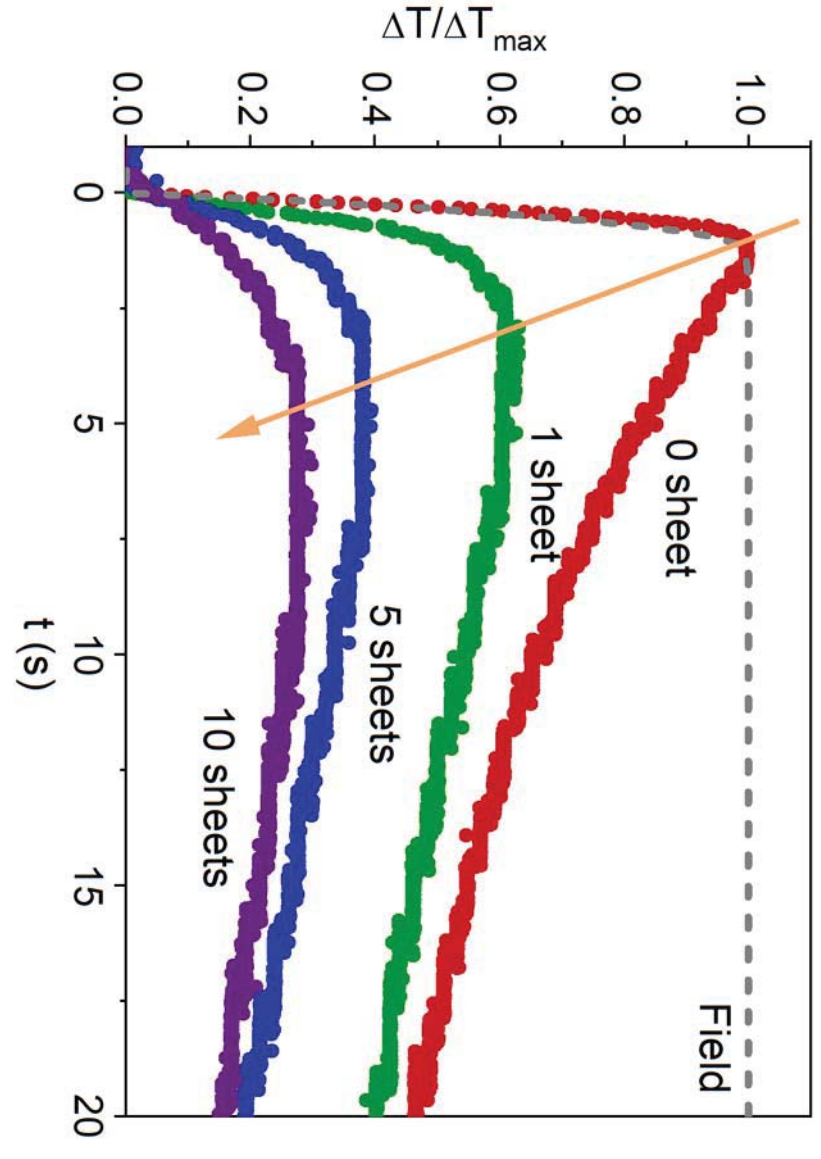

AIP Publishing
Journal of Applied Physics
ACCEPTED MANUSCRIPT

PLEASE CITE THIS ARTICLE AS DOI: 10.1063/5.0002870

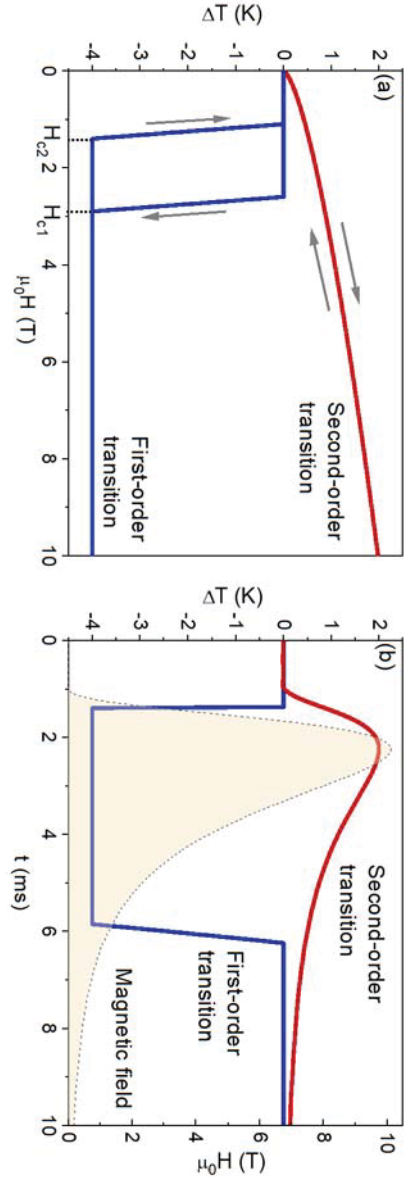

AIP Publishing
Journal of Applied Physics
ACCEPTED MANUSCRIPT

PLEASE CITE THIS ARTICLE AS DOI: 10.1063/5.0002870

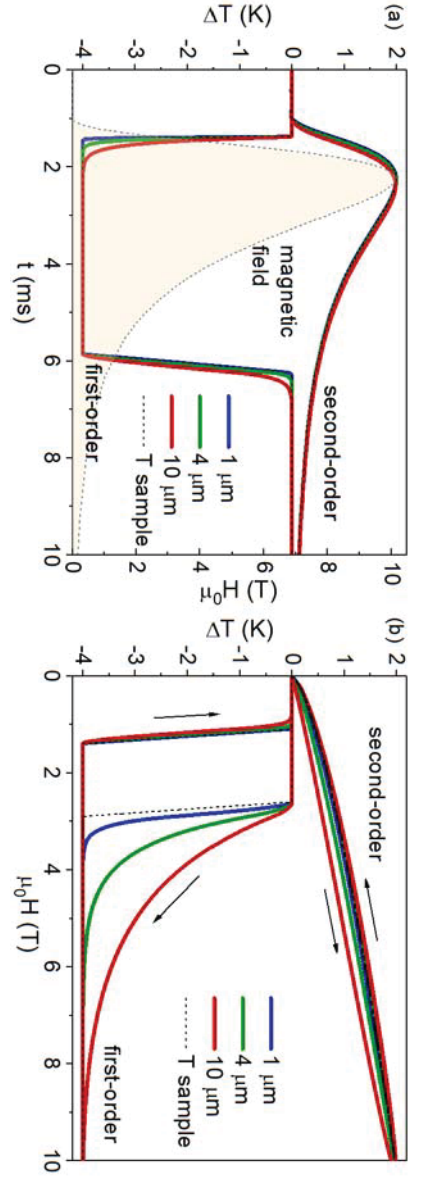

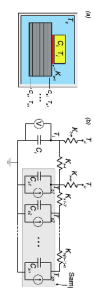

AIP Publishing Journal of Applied Physics

PLEASE CITE THIS ARTICLE AS DOI: 10.1063/5.0002870